INTERNATIONAL JOURNAL FOR NUMERICAL METHODS IN FLUIDS
Int. J. Numer. Meth. Fluids 2008; **58**:1223–1236
Published online 28 April 2008 in Wiley InterScience (www.interscience.wiley.com). DOI: 10.1002/fld.1789

Application of local DFD method to simulate unsteady flows around an oscillating circular cylinder

Y. L. Wu[1,2] and C. Shu[2,*,†]

[1]*Institute of High Performance Computing, 1 Science Park Road, #01-01 The Capricorn Singapore Science Park II, Singapore 117528*
[2]*Department of Mechanical Engineering, National University of Singapore, 10 Kent Ridge Crescent, Singapore 117576, Singapore*

SUMMARY

In this paper, the recently proposed local domain-free discretization (DFD) method is applied to simulate incompressible flows around an oscillating circular cylinder. It is found that it is very easy for the local DFD method to handle such moving boundary flow problems. This is because it does not need to move the mesh, which is indeed needed in traditional methods. Numerical experiments show that the present numerical results agree very well with the available data in the literature, and that the local DFD method is an effective tool for the computation of moving boundary flow problems. Copyright © 2008 John Wiley & Sons, Ltd.

Received 20 August 2007; Revised 28 January 2008; Accepted 29 January 2008

KEY WORDS: local DFD method; Cartesian mesh; moving boundary problem; flow pass the oscillating circular cylinder

1. INTRODUCTION

Currently, one of big challenges in computational fluid dynamics is to simulate flows around moving bodies in a complex domain. Basically, there are two ways to solve this problem. One way is to use the fixed reference frame (inertial reference frame), whereas the other is to move the reference frame with the moving body (accelerated reference frame). For the first way, continuous re-meshing around the body [1] is needed, which could be very laborious. In practice, the second way is usually adopted. In this case, the reference system is actually an accelerated reference

*Correspondence to: C. Shu, Department of Mechanical Engineering, National University of Singapore, 10 Kent Ridge Crescent, Singapore 117576, Singapore.
†E-mail: mpeshuc@nus.edu.sg

Contract/grant sponsor: Ministry of Education of Singapore; contract/grant number: R-265-000-182-112

system associated with the moving body. The disadvantage of this way is that it can be very difficult to apply to problems where there are more than one bodies in the flow domain moving at different speeds.

The recently proposed local domain-free discretization (DFD) method [2] is an efficient discretization approach. In this method, the body-fitted grid generation and coordinate transformation, which are necessary for the traditional numerical methods such as finite difference (FD) and differential quadrature methods to solve problem with irregular geometry, are totally avoided. The basic idea of DFD is inspired from the analytical method. That is, the discrete form of given partial differential equations (PDEs) can be independent from the solution domain. Its process may involve some points that may not be the mesh nodes and can be inside or outside the solution domain. The functional values at those points can be evaluated by approximate forms of solution along a line. In the local DFD method, all numerical work including discretization of derivatives and approximate form of solution for interpolation/extrapolation is made locally by using low-order polynomials, and any problem is solved in the Cartesian coordinate system. Therefore, in this sense, it is a kind of Cartesian mesh solver. It can also combine with the stencil adaptive mesh refinement technique [3] to effectively and accurately simulate the flow problem.

As a kind of Cartesian mesh solver, the local DFD method can easily handle the moving boundary problem. The basic mesh is fixed. When the boundary is moved, only the distance between the boundary nodes and the mesh points is changed, and this only affects the approximate form of solution to evaluate functional values at mesh points near the boundary. This process can greatly save the computational effort. In fact, in the local DFD method, all the mesh points can be classified into three categories. Category 1 is the interior point where numerical discretization of governing equations is needed. Category 2 is the outside point near the boundary where its functional value is obtained from the approximate form of solution. Category 3 is the outside point where nothing is needed to be done. When the embedded body is moved, the status (category) of mesh points will be changed. If we make sure that the change of status of mesh points is not jumped, that is, the status can only be changed from Category 1 to Category 2 or Category 2 to Category 3 and *vice versa*, the simulation of the moving boundary flow problem can be done using exactly the same way as for the stationary flow problem. For example, when the status is changed from Category 2 to Category 1, the points that are outside of the domain in the previous step now become the interior points where numerical discretization of governing equations needs the information of functional values at the previous step. Indeed, this information is available in the previous step by the approximate form of solution. Therefore, no additional work is needed.

To show the capability of the local DFD method for the simulation of the moving boundary flow problems, the unsteady flow around a cylinder oscillating laterally (cross-flow) in a free stream is considered. This kind of problem has been studied by many investigators such as Bishop and Hassan [4], Koopman [5], Lu and Dalton [6] and Guilmineau and Queutey [7]. Tang and Ingham [8, 9] solved this problem by using the FD scheme and the series expansion method. Chang and Chern [10] applied the vortex method to simulate the flow around an impulsively started circular cylinder. Dennis *et al.* [11] used the spectral-FD method to simulate the flow induced by a rotationally oscillating and translating circular cylinder. Recently, Liu *et al.* [12] solved this problem by using the spectral difference method. In general, for the moving boundary flow problem, the above numerical methods need tedious coordinate transformation or moving mesh technique. As will be shown in this work, the local DFD method can easily solve the moving boundary flow problem without introducing any coordinate transformation. And numerical

DOI: 10.1002/fld

experiments show that the present numerical results agree very well with the available data in the literature.

2. LOCAL DFD METHOD FOR THE MOVING BOUNDARY FLOW PROBLEM

The details of local DFD method can be found in the work of Shu and Wu [2]. In the following, the procedure of the local DFD method to handle the moving boundary problem on the Cartesian mesh is described.

As shown in Figure 1, the solid curve represents the location of the moving boundary at the current step, whereas the dashed curve shows the location of the boundary in the next or the previous step.

2.1. Local DFD method

Firstly, we give a brief description on the local DFD method. For simplicity, we assume that the mesh is uniform, and the mesh spacing in both the x- and y-directions is the same. Suppose that the solution of a problem is expressed by $f(x, y)$ in the Cartesian coordinate system. As shown in Figure 1, for the current step (the boundary is represented by solid curve), the mesh nodes inside the physical domain (interior mesh nodes) are represented by the solid circles, whereas the mesh nodes outside the domain are represented by open circles (such as node $A2$). The open squares represent the points intersected by the perpendicular line to the boundary (through $A2$) and the boundary curve and the mesh lines, such as points $P1$, $P2$, $P3$.

For the nodes far away from the boundary, such as node $C0$, the derivatives of PDEs can be discretized directly by the central difference scheme without any difficulty. For numerical discretization of derivatives at the nodes near the boundary such as $B2$, the local DFD method is applied. According to the DFD method, the discrete form of PDEs can involve some nodes outside the solution domain, and the functional values at these outside nodes such as node $A2$ can be

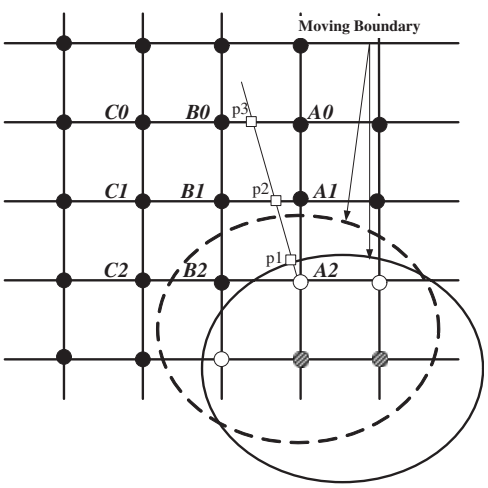

Figure 1. Configuration of the DFD-Cartesian mesh method for the moving boundary problem.

DOI: 10.1002/fld

computed by using local low-order approximate form of solution. Therefore, the central difference scheme on the uniform mesh can still be used by the local DFD method.

For example, the discrete form of the first- and second-order derivatives, respectively, in the x-direction at the position $B2$ can be approximated by

$$\frac{\partial^2 f_{B2}}{\partial x^2} = \frac{1}{h^2}[f_{A2} - 2f_{B2} + f_{C2}] + o(h^2) \tag{1}$$

$$\frac{\partial f_{B2}}{\partial x} = \frac{1}{2h}[f_{A2} - f_{C2}] + o(h^2) \tag{2}$$

where h is the mesh spacing on the uniform mesh in the x-direction, and $o(h^2)$ denotes the second order of the accuracy.

To evaluate the function value at point $A2$, the local polynomial extrapolation is used by adopting the variable values at the points $P1$, $P2$, $P3$ that are the intersection points of the line at the normal direction to the boundary $\vec{n}$ through $A2$ and the grid lines, as shown in Figure 1. In fact, there are many choices to do extrapolation. For example, we can take the mesh nodes $C2$, $B2$, and the intersection points of the x-coordinate line through $A2$ and the boundary curve, as done in Reference [2]. The reason of using the points along the line at the normal direction to the boundary $\vec{n}$ through $A2$ is to guarantee the unique function value at the mesh node for the discretization in the next time step. Thus, the variable value of the mesh node outside of the domain $A2$ can be obtained by extrapolation with the following three points extrapolation form:

$$f_{A2} = \frac{(r_{A2}-r_{P2})(r_{A2}-r_{P3})}{(r_{P1}-r_{P2})(r_{P1}-r_{P3})} f_{P1} + \frac{(r_{A2}-r_{P3})(r_{A2}-r_{P1})}{(r_{P2}-r_{P3})(r_{P2}-r_{P1})} f_{P2} + \frac{(r_{A2}-r_{P1})(r_{A2}-r_{P2})}{(r_{P3}-r_{P1})(r_{P3}-r_{P2})} f_{P3} \tag{3}$$

where r is the distance from the certain point to mesh node $A2$, an example being $r_{P2} = \sqrt{(x_{P2}-x_{A2})^2 + (y_{P2}-y_{A2})^2}$. The functional values at the points $P2$ and $P3$ can be calculated directly by interpolation between nodes $A1$ and $B1$ (for point $P2$), nodes $A0$ and $B0$ (for point $P3$). The functional value of the boundary point $P1$ is obtained from the boundary condition. The details on the implementation of boundary conditions are described in Section 2.4.

2.2. Identifying category of mesh nodes

As indicated in the Introduction, in the application of local DFD method to the moving boundary flow problem, all the mesh nodes can be classified into three categories. Category 1 (solid circle in Figure 1) is the interior node where the governing equation should be discretized. Category 2 (open circle in Figure 1) is the outside point near the boundary where its functional value is obtained from the approximate form of solution. Category 3 (shade circle in Figure 1) is the outside point where nothing is needed to be done. Thus, an important step is to identify the category of each mesh node.

As shown in Reference [2], the mesh nodes with Categories 1 and 3 are identified firstly by using the so-called 'odd/even parity method', which is inspired from the scan-line polygon fill algorithm in computer graphics. The 'odd/even parity method' is illustrated in Figure 2. Initially, all the mesh nodes are set to belong to Category 1. Suppose that there is a scan-line $i1$ in the horizontal direction. This line has four intersection points with solid body (denoted by Ω), which are represented as $p1$, $p2$, $p3$, $p4$. It was found that the odd index of intersection points such as $p1$, $p3$ is always the point where the scan-line moves in the body, whereas the even index of

DOI: 10.1002/fld

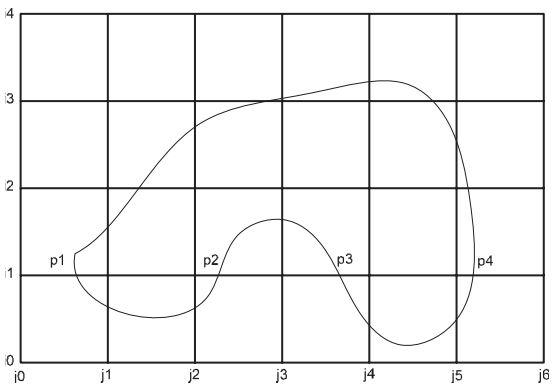

Figure 2. Illustration of 'odd/even parity method'.

the intersection points such as $p2$, $p4$ is the point where the scan-line moves out of the body. Therefore, we can number the series of intersection points in forward sequence along the scan direction and mark the mesh nodes between every odd/even parity as Category$(i1, j1 \sim j2) = 3$ and Category$(i1, j4 \sim j5) = 3$ as shown in Figure 2. We found that this method can determine the Category 3 of mesh nodes in the whole domain very quickly.

After identifying Categories 1 and 3 mesh nodes, Category 2 of mesh nodes can be determined by finding the mesh nodes belonging to Category 3 but with Category 1 nodes as its neighbors.

2.3. Local DFD method for the moving boundary flow problem

As shown in Figure 1, for the moving boundary problem, the position of the boundary in the current step is represented by the solid curve, and the boundary in the last time step is represented by the dashed curve. The mesh node $B2$ in the last time step is the node outside of the domain. However, for the current time step, $B2$ becomes the node inside of the domain where numerical discretization of governing equations is needed. For the unsteady flow problem, the function value at $B2$ in the last time step is needed when the time derivative is discretized. This is not a difficulty for the local DFD method where the functional value at $B2$ in the last time step has been known from extrapolation.

If the dashed curve denotes the boundary in the next time step, the solid curve still denotes the current time step. Then the mesh node $B2$ in the current time step is inside the solution domain, but for the next time step, $B2$ will become the node outside of the domain. As numerical discretization is only needed at the interior node, there is no need to store the solution at the current time step. The value at $B2$ in the next time step can be approximated by the local DFD method using Equation (3).

It is obvious that the local DFD method is very convenient for the moving boundary problem as long as the distance that the boundary moves is not larger than one nodal space in one time step. This is because we need the solution at some nodes that are the nodes outside of the domain in the last time step but are the nodes inside of the domain at the current time step. In the local DFD method, only for the outside nodes near the boundary within one nodal space, their function

DOI: 10.1002/fld

values are available from extrapolation. Therefore, the time step has to be small enough to make sure that the moving body sweeps across less than one mesh spacing.

2.4. Boundary conditions on the moving boundary

Velocity boundary conditions. For the incompressible flow, the nonslip condition is applied. For instance, if the body is static in the flow domain, the velocity at the node $P1$ is zero. For the moving boundary problem, the velocity at $P1$ is the same as the solid boundary velocity.

Pressure boundary conditions. The surface pressure can be determined from the normal momentum equation. For the incompressible flow, the gradient of the pressure along the normal direction can be expressed as

$$\frac{\partial p}{\partial \eta} = \frac{1}{Re}\frac{\partial^2 u_\eta}{\partial \eta^2} - \rho\frac{u_\xi^2}{R} \tag{4}$$

where R is the local curvature radius.

For details of implementing Equation (4) in the local DFD method, one can refer to the work of Shu and Wu [2].

In the practical computation, we found that it is important to enforce the continuity equation on the solid boundary. This is because the local DFD discretization is implemented on the nonstaggered grid. Therefore, the continuity equation on the solid boundary is not automatically satisfied. When this condition is not satisfied, it implies that the boundary is porous and there exists mass flux flow in or flow out through the boundary. This situation means the change of the physical problem. To avoid this situation, continuity equation should be accurately enforced on the nonporous solid boundary, i.e. for the incompressible flow, we have

$$\frac{\partial(\mathbf{u}\cdot\mathbf{n})}{\partial n} = 0 \tag{5}$$

where $\mathbf{n}$ is the normal direction to the boundary surface.

3. APPLICATION OF LOCAL DFD METHOD TO SIMULATE THE FLOW PAST AN OSCILLATING CIRCULAR CYLINDER

The problem of a cylinder oscillating laterally (cross-flow) in a free stream is a well-known moving boundary flow problem. There are various experimental and numerical investigations available. In the work of Lu and Dalton [6] and Guilmineau and Queutey [7], a reference frame fixed with the circular cylinder is used. Therefore, for a moving cylinder, it is an accelerated reference system. We have indicated in the Introduction that this treatment can be hardly applied to the problem in which there are more than one bodies inside the domain moving at different speeds.

This difficulty can be overcome by the local DFD method. The local DFD method uses the fixed reference frame, and the mesh is fixed. The internal objects are allowed to move freely through the mesh. In the process of applying the local DFD method, no body-fitted mesh generation and corresponding coordinate transformations are needed.

DOI: 10.1002/fld

3.1. Governing equations and boundary conditions

The unsteady incompressible Navier–Stokes equations in the Cartesian coordinate system are taken as the governing equations for the problem, which are expressed as

$$\frac{\partial u}{\partial x}+\frac{\partial v}{\partial y}=0 \tag{6}$$

$$\frac{\partial u}{\partial t}+u\frac{\partial u}{\partial x}+v\frac{\partial u}{\partial y}=-\frac{\partial p}{\partial x}+\frac{1}{Re}\nabla^2 u \tag{7}$$

$$\frac{\partial v}{\partial t}+u\frac{\partial v}{\partial x}+v\frac{\partial v}{\partial y}=-\frac{\partial p}{\partial y}+\frac{1}{Re}\nabla^2 v \tag{8}$$

where u and v are the dimensionless velocity components along the x- and y-directions, respectively. Re is the Reynolds number, p is the dimensionless pressure, and the Laplace operator ∇^2 is

$$\nabla^2=\frac{\partial^2}{\partial x^2}+\frac{\partial^2}{\partial y^2}$$

The circular cylinder is moved vertically with the speed v_T:

$$v_T=\frac{\mathrm{d}y_\mathrm{e}}{\mathrm{d}t} \tag{9}$$

where $y_\mathrm{e}=A_\mathrm{e}\sin(2\pi f_\mathrm{e}t)$, with A_e and f_e as the oscillating amplitude and frequency, respectively.

The boundary conditions of the problem are

(i) *uniform flow at the in-flow boundary*:

$$\begin{aligned} u&=1\\ v&=0 \end{aligned} \tag{10}$$

(ii) *no slip on the surface of the cylinder*:

$$\begin{aligned} u&=0\\ v&=0 \end{aligned} \tag{11}$$

(iii) *uniform flow at infinity except for the downstream boundary*:

$$\begin{aligned} u&=1\\ v&=0 \end{aligned} \tag{12}$$

(iv) *natural* (*zero-gradient*) *boundary condition at the downstream boundary*:

$$\begin{aligned} \frac{\partial u}{\partial x}&=0\\ \frac{\partial v}{\partial x}&=0 \end{aligned} \tag{13}$$

DOI: 10.1002/fld

3.2. Numerical discretization

It is found from the governing equations (6)–(8) that an independent equation for the pressure is absent. To resolve this problem, the projection method [13] is employed in the present work. In this paper, the time derivatives in Equations (7)–(8) are approximated by the three-step third-order Runge–Kutta method. For a time increment $\Delta t = t^{n+1} - t^n$, numerical discretization consists of the following three steps:

Step 1:

$$\frac{\mathbf{u}^{n+1/3} - \mathbf{u}^n}{\Delta t/3} = -H(\mathbf{u}^n) - G(p^n) + \frac{1}{Re} L(\mathbf{u}^n) \tag{14}$$

Step 2:

$$\frac{\mathbf{u}^{n+1/2} - \mathbf{u}^n}{\Delta t/2} = -H(\mathbf{u}^{n+1/3}) - G(p^n) + \frac{1}{Re} L(\mathbf{u}^{n+1/3}) \tag{15}$$

Step 3:

$$\frac{\mathbf{u}^* - \mathbf{u}^n}{\Delta t} = -H(\mathbf{u}^{n+1/2}) + \frac{1}{Re} L(\mathbf{u}^{n+1/2}) \tag{16}$$

where H denotes the discrete advection operator, G is the discrete gradient operator, and L is the discrete Laplacian operator. Superscripts $n, n+1/2, n+1/3$, and $n+1$ denote the time levels, and $\mathbf{u}^*$ is the intermediate velocity. The final velocity $\mathbf{u}$ at t^{n+1} is corrected by including the pressure field, given as

$$\frac{\mathbf{u}^{n+1} - \mathbf{u}^*}{\Delta t} = -Gp^{n+1} \tag{17}$$

Combining the continuity equation

$$D\mathbf{u}^{n+1} = 0 \tag{18}$$

and taking the divergence of Equation (17), the pressure Poisson equation is derived to correct the velocity equation as

$$Lp^{n+1} = \frac{1}{\Delta t}(D\mathbf{u}^*) \tag{19}$$

where D is the divergence operator. Finally, the velocity $\mathbf{u}^{n+1}$ is updated by the solution of pressure equation (17):

$$\mathbf{u}^{n+1} = \mathbf{u}^* - \Delta t G(p^{n+1}) \tag{20}$$

In the local DFD method, the second-order central difference scheme is applied in both the x- and y-directions to approximate the spatial derivatives, including all the discrete operators. Suppose that at a mesh node (x_i, y_j), if one or more of nodes $(i-1, j), (i+1, j), (i, j-1), (i, j+1)$ (i.e. the neighboring nodes of mesh node (x_i, y_j)) are not located in the physical domain, then the functional values at those nodes are evaluated by using Equation (3).

DOI: 10.1002/fld

3.3. Numerical results and discussions

The computational domain is shown in Figure 3, where a is the radius of the cylinder. An initial uniform Cartesian mesh with the introduction of stencil refinement technique [3] (54 002 nodes in total) is used (see Figure 4). Note that the nodes are distributed to cover the area where the oscillating cylinder moves across. To make sure that the moving distance of each node in one time step is less than nodal distance, the time interval should be small enough.

3.3.1. Fixed cylinder case. This case has been studied by many researchers [6, 7, 14, 15]. The simulation of the two-dimensional flow past a fixed cylinder at the Reynolds number of $Re = 185$

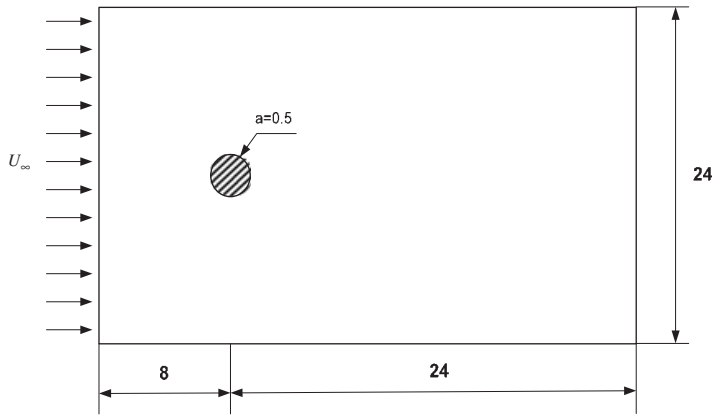

Figure 3. Computational domain for simulation of the flow around a circular cylinder.

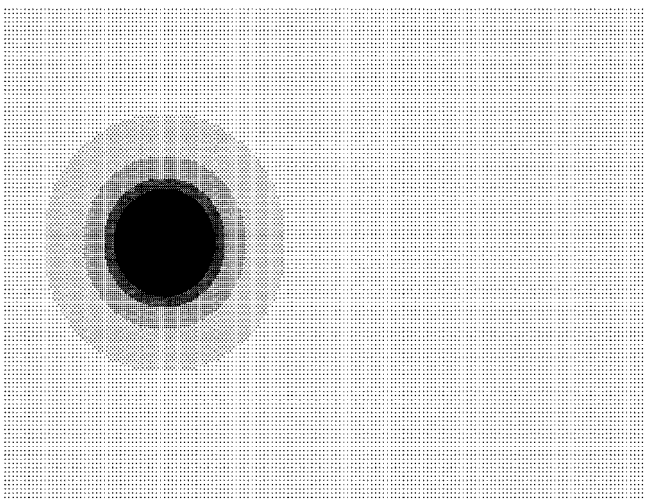

Figure 4. Node distribution for the problem.

DOI: 10.1002/fld

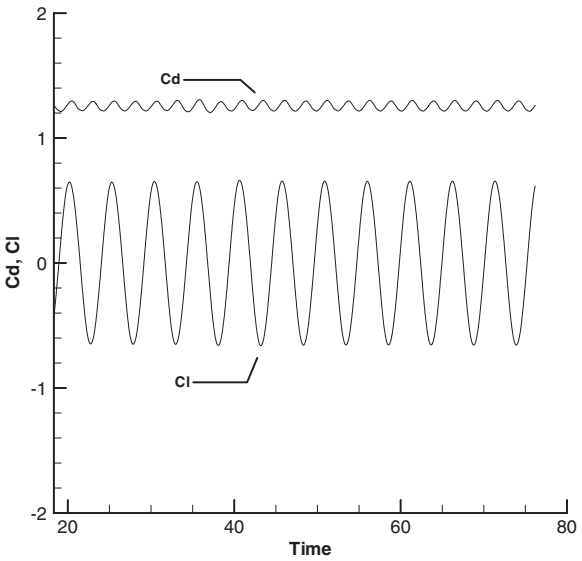

Figure 5. The time evolution of lift and drag coefficients for $Re = 185$.

Table I. Numerical and experimental values of $\overline{C}_d$, $C_{Lr.m.s.}$ and St at $Re = 185$ (fixed cylinder case).

Work	$\overline{C}_d$	$C_{Lr.m.s.}$	St
Lu and Dalton [6]	1.31	0.422	0.195
Guilmineau and Queutey [7]	1.287	0.443	0.195
Present	1.255	0.463	0.195

is used as a test case to compare with other numerical and experimental results for the validation of the present method.

Figure 5 shows the time histories of the lift and drag coefficients for nonoscillating cylinder at $Re = 185$. The average drag coefficient, $\overline{C}_d$, the r.m.s. value of the lift coefficient, and the Strouhal number, St, are reported in Table I. They are compared with other experimental and numerical results in the literature. The agreement is quite good. It means that the local DFD method with stencil refinement technique works very well for the fixed cylinder case. The following section will show its performance for the moving boundary problem, i.e. the flow past the oscillating cylinder.

3.3.2. Oscillating cylinder case. Flow past a transversely oscillating circular cylinder is a good benchmark case to validate the computational techniques for the moving boundary problem. This problem has been investigated by many researchers, and the associated synchronization phenomenon is observed in the wake of the cylinder and refers to the situation where the frequency of vortex shedding in the wake synchronizes with the frequency of an imposed perturbation. This kind of synchronization occurs around $f_e/f_0 \sim 1$, where f_e is the excitation frequency and f_0 is the vortex-shedding frequency from the stationary cylinder.

DOI: 10.1002/fld

In this work, we have performed calculations for $Re=185$, $A_e/D=0.2$, where D is the diameter of the cylinder. The range of $f_e/f_0=1.1, 1.12, 1.2$ is considered. Each of these simulations is integrated in time for about 150 nondimensional time units, which is sufficient to reach a stable state.

At first, we conduct the grid-independent and time-step-independent study on the personal computer (Intel P4, 2.4 GHz processor, 512 MB of RAM). For the grid-independent study, three grids are taken. Each grid is generated from a background mesh with local refinement level by level [2]. The finest mesh is placed near the solid boundary. For all the three grids, the background mesh is the same, that is 161×121. Grid 1 takes 6 levels of local mesh refinement with 36 155 mesh nodes in total, whereas Grid 2 adopts 8 levels of local mesh refinement with 54 002 mesh nodes in total. Grid 3 has 10 levels of local mesh refinement with 87 557 mesh nodes in total. The time average of drag coefficient, the r.m.s. value of the lift coefficient, and the Strouhal number, St, at the excitation frequency of $f_e/f_0=1.1$ for the three grids are shown in Table II. It can be seen from Table II that with increase in mesh nodes, the difference of numerical results becomes smaller and smaller, and Grid 2 can provide accurate results. Thus, in the following computations, Grid 2 is adopted. For the time-step-independent study, two time steps are used. They are $h=0.0025$ and 0.005. Numerical results of these two time steps are also shown in Table II. It is found that their differences are within 2%. Therefore, in the following simulations, we take h as 0.005. Table II also shows the results of Guilmineau and Queutey [7] for comparison. Obviously, the present results agree very well with those of Guilmineau and Queutey [7].

Figures 6–8 display the drag and lift coefficients for different values of f_e/f_0. The results of Guilmineau and Queutey [7] are also shown in the figures for comparison. Obviously, the present results and those of Guilmineau and Queutey [7] show the same flow pattern. It is found that the drag and lift coefficients exhibit regular signs of the influence of a higher harmonic wave. As the excitation frequency increases, the beating frequency decreases.

Figure 9(a) shows the instantaneous streamlines when the oscillating cylinder is at the extreme upper position for the case $f_e/f_0=1.1$. The figure shows two saddle points in the form of intersecting streamlines. The centers of the closed streamlines suggest the existence of vorticity concentrations in those regions. This concentration of vorticity involves the entire near wake and results in a tighter vortex structure. The corresponding contours of vorticity are given in Figure 9(b). The upper vortex has been diminished in strength to the extent that the lower vortex has become the dominant vortex and the upper vortex has rolled up tightly behind the cylinder.

Table II. Comparison of $\overline{C}_d$, $C_{Lr.m.s.}$ and St at $Re=185$, $A_e/D=0.2$, $f_e/f_0=1.1$ (oscillating cylinder case).

		$\overline{C}_d$	$C_{Lr.m.s.}$	St
Present method with grid-independent study	Grid 1	1.412	0.747	0.240
	Grid 2	1.484	0.875	0.214
	Grid 3	1.454	0.854	0.214
Present method with time-step-independent study (Grid 2)	$\Delta t=0.005$	1.484	0.875	0.214
	$\Delta t=0.0025$	1.466	0.865	0.214
Guilmineau and Queutey [7] (mesh $=240\times200$)		1.420	0.897	0.214

Grid 1: background mesh 161×121 with 6 levels of mesh refinement and 36 155 mesh nodes in total. Grid 2: background mesh 161×121 with 8 levels of mesh refinement and 54 002 mesh nodes in total. Grid 3: background mesh 161×121 with 10 levels of mesh refinement and 87 557 mesh nodes in total.

DOI: 10.1002/fld

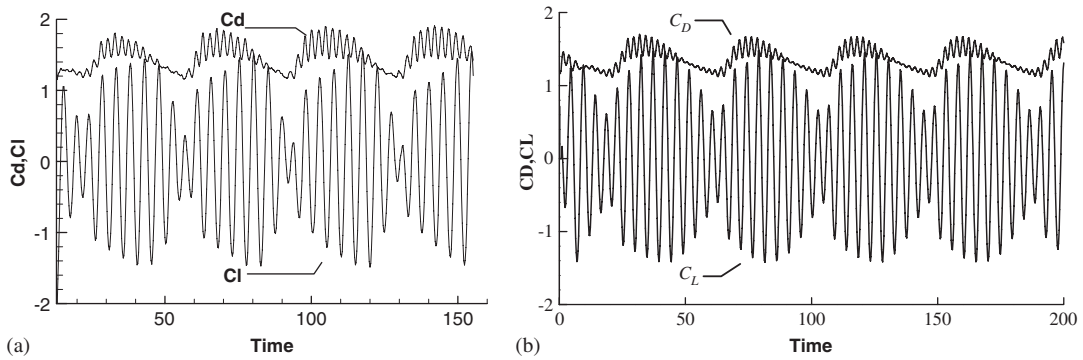

Figure 6. Drag and lift coefficients *versus* time for $Re = 185$ and $A_e/D = 0.2$ for $f_e/f_0 = 1.10$: (a) present study and (b) Guilmineau and Queutey [7].

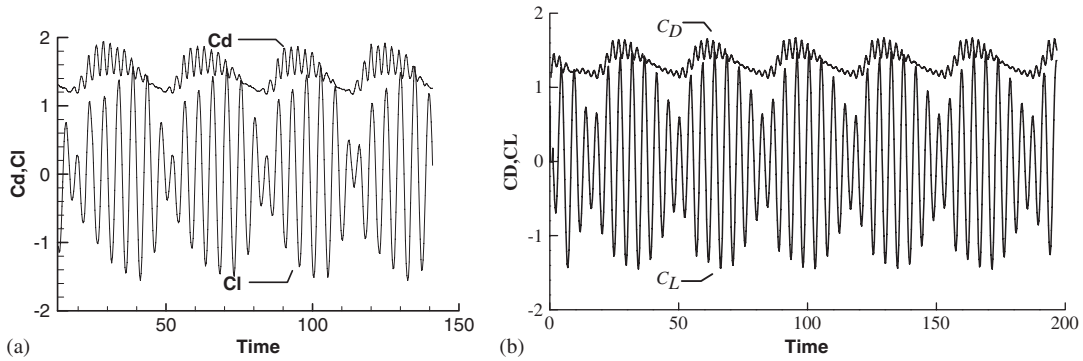

Figure 7. Drag and lift coefficients *versus* time for $Re = 185$ and $A_e/D = 0.2$ for $f_e/f_0 = 1.12$: (a) present study and (b) Guilmineau and Queutey [7].

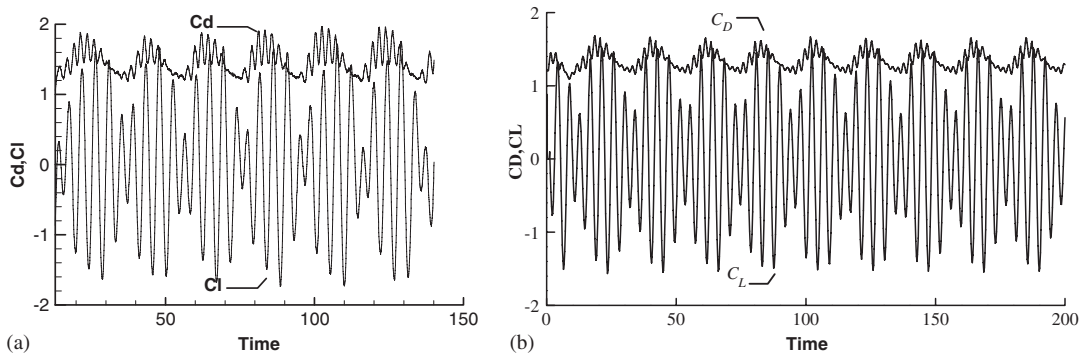

Figure 8. Drag and lift coefficients *versus* time for $Re = 185$ and $A_e/D = 0.2$ for $f_e/f_0 = 1.20$: (a) present study and (b) Guilmineau and Queutey [7].

DOI: 10.1002/fld

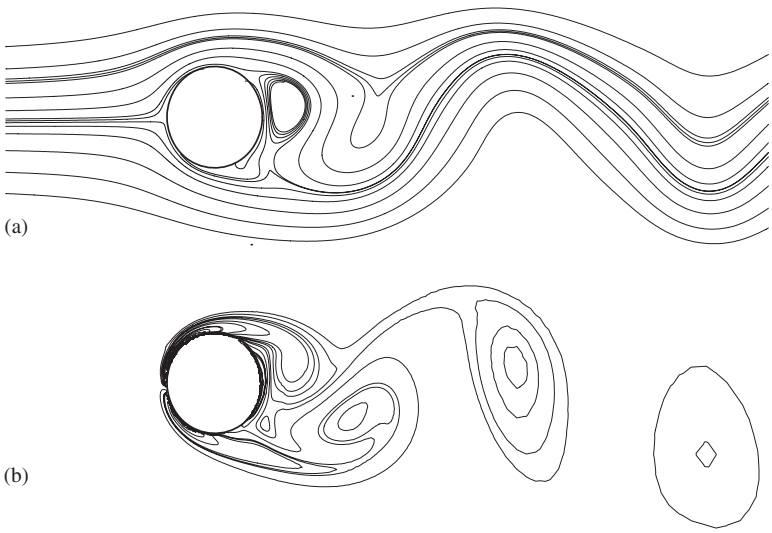

Figure 9. Instantaneous streamlines and vorticity contours for $Re=185$ and $A_e/D=0.2$, $f_e/f_0=1.10$. The location of the cylinder is at its extreme upper position: (a) streamlines and (b) vorticity contours.

4. CONCLUSIONS

The advantages of the local DFD method for the simulation of the moving boundary flow problems are demonstrated in this paper. In the local DFD method, the mesh generation and numerical discretization over the mesh nodes are totally unrelated to the internal bodies in the domain. The moving boundary condition only affects the calculation of functional values at the nodes outside of the domain via the extrapolation process. The application of the present method to simulation of flows past an oscillating cylinder shows good agreement with the numerical flow predictions in the literature. In the present work, the local DFD method is applied with mesh refinement technique. It is expected that for the high Reynolds number case, more mesh refinement near the solid boundary is needed to capture the thin boundary layer, and the upwind differencing may be required to enhance the numerical stability.

ACKNOWLEDGEMENTS

This work was supported by the Academic Research Fund (AcRF Tier 2) of Ministry of Education of Singapore (R-265-000-182-112).

REFERENCES

1. Tezduyar TE, Behr M, Liou J. A new strategy for finite element computations involving moving boundaries and interfaces—the deforming-spatial-domain/space–time procedure: I. The concept and the preliminary numerical tests. *Computer Methods in Applied Mechanics and Engineering* 1992; **94**:353.
2. Shu C, Wu YL. Adaptive mesh refinement-enhanced local DFD method and its application to solve Navier–Stokes equations. *International Journal for Numerical Methods in Fluids* 2006; **51**:897–912.
3. Ding H, Shu C. A stencil adaptive algorithm for finite difference solution of incompressible viscous flows. *Journal of Computational Physics* 2006; **214**:397–420.

DOI: 10.1002/fld

4. Bishop RED, Hassan AY. The lift and drag forces on a circular cylinder oscillating in a flowing fluid. *Proceedings of the Royal Society of London*, *Series A* 1964; **277**:51–75.
5. Koopman GH. The vortex wakes of vibrating cylinders at low Reynolds numbers. *Journal of Fluid Mechanics* 1967; **28**:501–512.
6. Lu XY, Dalton C. Calculation of the timing of vortex formation from an oscillating cylinder. *Journal of Fluids and Structures* 1996; **10**:527–541.
7. Guilmineau E, Queutey P. A numerical simulation of vortex shedding from an oscillating circular cylinder. *Journal of Fluids and Structures* 2002; **16**:773–794.
8. Tang T, Ingham DB. On steady flow past a rotating circular cylinder at Reynolds numbers 60 and 100. *Computers and Fluids* 1991; **19**:217–230.
9. Ingham DB, Tang T. A numerical investigation into the steady flow past a rotating circular cylinder at low and intermediate Reynolds numbers. *Journal of Computational Physics* 1990; **87**:91–107.
10. Chang CC, Chern RL. A numerical study of flow around an impulsively started circular cylinder by a deterministic vortex. *Journal of Fluid Mechanics* 1991; **233**:243–263.
11. Dennis SCR, Kocabiyik S, Nguyen P. The flow induced by the rotationally oscillating and translating circular cylinder. *Journal of Fluid Mechanics* 2000; **407**:123–143.
12. Liu Y, Shu CW, Tadmor E, Zhang M. Non-oscillatory hierarchical reconstruction for central and finite volume schemes. *Communications in Computational Physics* 2007; **2**:933–963.
13. Young DL, Huang JL, Eldho TI. Simulation of laminar vortex shedding flow past cylinders using a coupled BEM and FEM model. *Computer Methods in Applied Mechanics and Engineering* 2001; **190**:5975–5998.
14. Dennis SCR, Chang GZ. Numerical solutions for steady flow past a circular cylinder at Reynolds numbers up to 100. *Journal of Fluid Mechanics* 1971; **42**:471.
15. Braza M, Chassaing P, Ha Minh H. Numerical study and physical analysis of the pressure and velocity fields in the near wake of a circular cylinder. *Journal of Fluid Mechanics* 1986; **165**:79.

DOI: 10.1002/fld